Binding of two zinc ions promotes liquid-liquid phase separation of Tau

Dahbia Yatoui, Philipp Tsvetkov, Romain La Rocca, Viktoriia Baksheeva, Diane Allegro, Gilles Breuzard, Géraldine Ferracci, Deborah Byrne, François Devred

Binding of two zinc ions promotes liquid-liquid phase separation of Tau

Dahbia Yatoui[1], Philipp O. Tsvetkov[1*], Romain La Rocca[1], Viktoriia E. Baksheeva[1], Diane Allegro[1], Gilles Breuzard[1], Géraldine Ferracci[1], Deborah Byrne[2], François Devred[1*]

[1] Aix Marseille Univ, CNRS, INP, Institute of Neurophysiopathol, Faculté des Sciences Médicales et Paramédicales, Marseille, France

[2] Institut de Microbiologie de la Méditerranée, CNRS, FR3479, Aix-Marseille Université, 13402 Marseille, France

Highlights

- Zinc is known to trigger tau aggregation and droplet formation.
- Three zinc-binding sites have been identified in a NMR study.
- We confirmed the presence of three distinct zinc binding sites on tau protein.
- Zinc binding site located in the R2R3 domain is crucial for tau aggregation.
- Zinc binding to only one site does not induce tau aggregation nor LLPS.
- Any two of three existing zinc-binding sites are necessary to induce droplets.
- We proposed a model of zinc-induced LLPS.

Abstract

Tau is a naturally disordered microtubule associated protein which forms intraneuronal aggregates in several neurodegenerative diseases including Alzheimer disease (AD). It was reported that zinc interaction with tau protein can trigger its aggregation. Recently we identified three zinc binding sites located in the N-terminal part, repeat region and the C-terminal part of tau. Here we characterized zinc binding to each of the three sites using isothermal titration calorimetry (ITC) and determined the impact of each site on aggregation using dynamic light scattering (DLS) assays. First, we confirmed the presence of three zinc binding sites on tau and determined the thermodynamic parameters of binding of zinc to these sites. We found a high-affinity zinc binding site located in the repeat region of tau and two N- and C-terminus binding sites with a lower binding constant for zinc. Second, we showed that tau aggregation necessitates zinc binding to the high affinity site in the R2R3 region, while LLPS necessitates zinc binding to any two binding sites. With regard to the role of zinc ions in the aggregation of proteins in neurodegenerative diseases, these findings bring new insights to the understanding of the aggregation mechanism of tau protein induced by zinc.

Keywords: tau protein; liquid-liquid phase separation; aggregation; zinc

Introduction

Tau is an intrinsically disordered microtubule associated protein that plays an important role in a number of vital processes via regulation of microtubule dynamics (Barbier et al. 2019). It binds tubulin, promotes its polymerization, and stabilizes formed microtubules. Besides its important physiological role, it is involved in the development of a number of neurodegenerative diseases such as Alzheimer's disease (AD), Parkinson's disease (PD) and frontotemporal lobar degeneration (FTD), also called tauopathies (Shelkovnikova et al. 2012). Tau is a major component of neurofibrillary tangles in AD, which consist of stacked paired helical filaments (PHF) of hyper-phosphorylated tau molecules (Ochalek et al. 2017) and also forms various types of intracellular aggregates in FTD and PD.

Dyshomeostasis of metal ions, in particular zinc, plays an important role in the development of neurodegenerative diseases (Wang et al. 2020). Indeed, zinc is directly involved in aggregation of a number of proteins associated with neurodegenerative diseases such as amyloid-β (Esler et al. 1996), FUS/TLS (Efimova et al. 2017), TDP-43 (Caragounis et al. 2010; Garnier et al. 2017) and tau (Mo et al. 2009). In particular, zinc has been shown to directly increase the toxicity of tau in cells (Huang et al. 2014) and to induce neuron death through the acceleration of tau aggregation (Hu et al. 2017; Li, Du, and Ni 2019). The direct effect of zinc on tau aggregation has also been confirmed with purified tau constructs (Mo et al. 2009; Jiji et al. 2017; Moreira et al. 2019). Recently, it was shown that zinc can induce the formation of reversible aggregates of tau (Roman et al. 2019), and can promote its liquid-liquid phase separation (LLPS) (Gao et al. 2022). Although tau aggregation and LLPS are two distinct processes, they seem to be strongly linked. Indeed, it was demonstrated that LLPS can initiate tau aggregation (Wegmann et al. 2018). Moreover, both processes are accelerated in the presence of zinc ions (Gao et al. 2022; Chowdhury, Roy Chowdhury, and Peter Lu 2022). Zinc ions bind to tau at three sites: one high-affinity site in the MTBR (microtubule binding region) and two lower affinity sites located in tau C- and N-terminal regions (La Rocca et al. 2022). However, it is not clear how these three Zn^{2+}-binding sites participate in LLPS and tau aggregation. We addressed this question by designing a set of tau constructs with different combinations of alanine mutants that allowed us to deactivate one or two of three zinc binding sites (Fig.1). We then used a combination of biophysical methods

including isothermal titration calorimetry (ITC), dynamic light scattering (DLS) and fluorescence microscopy to assess the role of each site in LLPS and tau aggregation.

Methods

Protein expression and purification - The full-length human tau and histidine mutants were cloned into the pET-3d vector and overexpressed in *Escherichia coli* BL21(DE3) strain. Bacterial cells were grown in LB “Conda" with 100 µg/ml ampicilline at 37°C and 150 rpm and induced using 0.5 mM IPTG for 3h hours at 37°C when the OD_{600} reached 0.6. Then the cells were pelleted and resuspended in a lysis buffer as previously described (Roman et al. 2019). After 2 cycles in French Press at 4 tonnes, non-thermostable proteins were precipitated at 90°C for 12 minutes. Lysates were then cleared by centrifugation at 43000 g for 30 minutes at 4°C. Supernatants were filtered through a 0.22 µm pore filter and loaded onto a 5 mL Hitrap SP Sepharose HP cation exchange column equilibrated in 45 mM MES pH 6.5. Tau protein was eluted using 50 mM MES, 500 mM, NaCl pH 6.5 at 1 mL/min; dialyzed for 2 hours then overnight at 4°C against 2 L of water in a 3.5 kDa MWCO membrane and dry-lyophilized. Before use, all tau samples were airfuged at 25 psi for 10 min and protein concentration was measured at 280 nm with an extinction coefficient of 7,700 $M^{-1}cm^{-1}$ with JASCO V-750 spectrophotometer.

Monitoring of LLPS - For microscopy experiments, proteins were labeled with Alexa fluor 488 Molecular Probes Kit (Invitrogen, Eugene, OR, USA) by adding 10 µL of the dye (10 mg/mL) dissolved in DMSO to 100 µL of tau (200 µM) in 0.1 M sodium bicarbonate buffer pH 8. The mixture was incubated at room temperature for 2 hours with stirring as described previously (Boyko et al. 2019). Excess dye was removed by overnight dialysis in 50 mM Tris, 1 mM TCEP buffer pH 7.5 at 4°C. Protein concentration and labeling efficiency was determined by measuring the absorbance at 280 nm and 495 nm. Samples were prepared by adding zinc ions at 400 µM final concentration to 50 µM labeled tau in 50 mM Tris, 1mM TCEP buffer pH 7.5. No zinc was added to control samples. 5 µL of the mixture were placed on the glass surface of 35 mm microdish (Ibis GmbH, Gräfelfing, Bayern, Germany) that was covered with a coverglass. The measurements were performed at 40°C within 10 min after the

addition of zinc using a ZEISS Laser Total Internal Reflection Fluorescence Imaging System TIRF 3 (Carl Zeiss, Germany) with an x100 oil immersion objective lens (1.46 numerical aperture).

Isothermal titration calorimetry (ITC) - Zinc binding to tau mutants was investigated using MicroCal PEAQ-ITC instrument (Malvern, Worcestershire, UK) at 10°C in 50 mM Tris buffer at pH 7.5 in the presence of 1 mM TCEP. Tau concentration in the calorimetric cell was 50 µM and zinc concentration in the syringe was 1 or 2 mM. Data were analyzed using MicroCal PEAQ-ITC analysis software and fitted with a one or two set of sites models. The thermodynamic parameters are the average of three different experiments.

Dynamic Light Scattering (DLS) - DLS measurements were carried out using a Malvern Zetasizer Nano ZS instrument at 40°C with a scattering angle of 173°. Tau was analyzed from 50 µM samples in 50 mM Tris, 1 mM TCEP, pH 7.5 in the absence or presence of 0, 50, 100, 200, and 400 µM $ZnCl_2$. Before use, samples of 100 µL were centrifuged at 14 000 rpm for 15 min at 4°C. The upper 50 µL of each sample were collected to be used for the experiment. For each assay three measurements were performed; each one consisting of 10-15 runs of 10 seconds. The resulting data were analyzed using Zetasizer software (version 7.12) (Malvern, Worcestershire, UK).

Results

Role of zinc binding sites in LLPS formation.

In order to investigate the impact of each zinc-binding site on the formation of zinc-induced LLPS, we have generated seven tau constructs with one (xoo-tau, oxo-tau, oox-tau), two (xxo-tau, xox-tau, oxx-tau) or three (xxx-tau) inactivated zinc-binding sites (Fig.1). The purified tau proteins were fluorescently labeled and incubated with zinc. The formation of tau-containing droplets in the absence and in the presence of zinc ions was shown using FRAP (Fig.S1) and monitored using fluorescence microscopy (Fig.2). In the presence of zinc ions, constructs with only one inactivated zinc-binding site (xoo-tau, oxo-tau, oox-tau) as well as wt-tau formed droplets with size ranging from 0.5 to 3 µm, typical for LLPS. When two or all three Zn^{2+}-binding sites were mutated, no LLPS was observed in the presence of Zn^{2+}. No droplets were observed in the absence of zinc ions for all constructs. Thus, any two Zn^{2+}-binding sites can mediate zinc-induced LLPS whereas one non-mutated Zn^{2+}-binding site is not sufficient to trigger droplet formation.

Mutation of two Zn-binding sites does not alter Zn binding to the third site

One possible explanation for absence of zinc-induced LLPS in tau constructs with only one non-mutated site (xxo-tau, xox-tau, oxx-tau) is that this site becomes non-functional when the two others are inactivated. To test this hypothesis and to investigate whether zinc still binds to tau when only one zinc-binding site is left, we used isothermal titration calorimetry (ITC). Titration of the xox-tau construct (C- and N-terminal Zn^{2+}-binding sites inactivated) by zinc ions revealed the existence of one site with association constant of 1.2×10^{6} M^{-1}, (Fig.3, Table 1). This data demonstrates that binding to C- and N-terminal sites is not a requirement for zinc interaction with the MTBR domain. Similarly, the titration of oxx-tau and xxo-tau constructs revealed that both C- and N-terminal binding sites are independent from other sites and are able to chelate one zinc ion each with similar 2.4×10^{4} M^{-1} and 3.3×10^{4} M^{-1} constants respectively (Fig.3, Table 1). Thus, the three zinc binding sites of tau are independent, as tau with any two inactivated zinc binding sites is still able to bind one zinc ion. Taken together, our results show that constructs with only one binding site are able to bind Zn, but are not capable of triggering zinc-induced LLPS.

Quantification of tau in LLPS.

While the results obtained by microscopy allowed us to show the presence of tau-containing droplets, they did not provide quantitative data nor did they give us information about tau monomers or small oligomers. We therefore used dynamic light scattering (DLS) to evaluate the size distribution of all tau forms and thus estimate the percentage of tau in droplet state. Figure 4 depicts typical DLS correlation curves of wt-tau and tau constructs at different zinc concentrations. Similar to the results from our microscopy experiments, the tau constructs with two functional Zn^{2+}-binding sites (oox, oxo, xoo) behaved drastically different from tau constructs with only one active Zn^{2+}-binding site (xxo, xox, oxx).

Addition of zinc ions did not change the DLS correlation curves for constructs with single N- or C-terminal Zn^{2+}-binding site (oxx-tau and xxo-tau) constructs even at large excess of zinc (Fig. 4E and F respectively), which is in agreement with our microscopy data. In contrast, the correlograms of xox-tau exhibited a slight but gradual appearance of a shoulder upon zinc increase indicating the presence of particles. Deconvolution of xox-tau correlograms in intensity distribution revealed that the particle size increased up to 1 µm at 8-fold excess of zinc (Fig. 5). Yet, deconvolution of correlograms in volume distribution revealed that less than 0.1% of the total amount of tau is contained in these particles (data not shown), explaining why they were not observed in our microscopy experiments.

In tau constructs with only one mutated -zinc-binding site (xoo-tau, oxo-tau, and oox-tau) a similar shoulder was observed up to a 2-fold excess of zinc and volume distribution demonstrated an increase of total amount of tau in droplets upto 0.7%. As zinc concentration was further increased, all three constructs exhibited a significant increase in size of particles by about three orders of magnitude (Fig. 5, Table 2), corresponding, as we demonstrated previously, to large aggregates (Roman et al. 2019). This means that while for the formation of droplets any two zinc binding sites are necessary, for the formation of larger aggregates, the R2R3-domain high affinity site is necessary.

This conclusion is consistent with the results depicted in Figure 5 that shows the evolution of average diameter of all species in the solution (Z-average) for all tau constructs upon rise of zinc concentration. Indeed, the average diameter of particles is much higher for wt-tau and the two single site mutants with functional zinc-binding site in the R2R3-domain (xoo-tau and oox-tau). These data also suggest that contrary

to droplets that contain only a small fraction of tau, the aggregates of wt-tau, xoo-tau, and oox-tau formed in the presence of large excess of zinc contain the majority of the tau. Since it was not possible to determine the amount of tau in the aggregates from DLS data due to method limitation, we estimated it by cosedimentation. We measured the concentration of tau in supernatant after centrifugation of tau solution in the presence of 8-fold excess of zinc and found about 70% of total tau (data not shown).

Discussion

Zinc is the most abundant trace element in the brain. Due to its implication in several physiological processes, keeping its level in physiological range is crucial for proper neuronal functioning (Portbury and Adlard 2017). Indeed, disruption of zinc homeostasis in the brain leads to many neurodegenerative and psychiatric disorders (Grabrucker, Rowan, and Garner 2011).

Despite the implication of both tau protein and zinc ions in the pathogenesis of several neurodegenerative disorders, the exact molecular mechanism of zinc-induced tau aggregation and formation of LLPS is still not completely elucidated. It was demonstrated that a zinc binding site is located in the microtubule binding domain region (MTBR) of tau. Two reports pointed out seven residues located in the R2-R3 repeat region of tau (C291, C322, H268, H299, H329, H330, and H362) that could participate in zinc binding (Mo et al. 2009; Hu et al. 2017). Recently, a model of zinc-induced tau aggregation proposed that tau molecules are linked together by zinc ions which are chelated by cysteine and histidine residues of MTBR of different tau monomers (Chowdhury, Roy Chowdhury, and Peter Lu 2022). However, this model did not take into account the two recently discovered zinc binding sites in C- and N-terminal domains of tau, which could also participate in tau aggregation and the formation of droplets (Roman et al. 2019; Moreira et al. 2019). The amino acids of these two sites have been recently identified by NMR (La Rocca et al. 2022). In this study, we systematically mutated all three Zn^{2+}-binding sites to create a set of different constructs with one or two deactivated sites in order to characterize each individual zinc binding to each site and to investigate their impact on the formation of both droplets and aggregates of tau.

Our study revealed several interesting results concerning the two recently discovered low affinity N- or C-terminal sites. First, both sites bind zinc with a similar association constant of $2.5\pm0.3\times10^{4}$ M^{-1}, as shown by ITC characterization of oxx-tau and xxo-tau mutants. Second, zinc binding to each of the three sites is independent from other sites. Third, a single N- or C-terminal site is not sufficient to induce Zn^{2+}-related LLPS or aggregation. Indeed, zinc binding to the two constructs xxo- and oxx-tau did not induce the formation of tau-containing droplets or large aggregates. These results are in agreement with the model proposed by Chowdhury and Lu (Chowdhury, Roy Chowdhury, and Peter Lu 2022), as both of these constructs lack the functional high-affinity binding site in the R2R3 region of tau. Fourth, even though individual N- or C-terminal sites are not sufficient to induce Zn^{2+}-related LLPS or aggregation, these sites are still necessary for these processes. Indeed, when the construct with both N- and C-terminal sites mutated (xox-tau) was used, we did not observe the formation of droplets by microscopy, nor the formation of large aggregates by DLS. Thus, contrary to the Chowdhury and Lu model, the high-affinity zinc-binding site cannot induce LLPS or aggregation by itself. Furthermore, using a set of constructs with only one deactivated site (xoo-tau, oxo-tau and oox-tau), we showed that at least two zinc-binding sites are necessary for zinc-induced liquid-liquid phase separation of tau. Indeed, all three mutants demonstrated the formation of droplets in the presence of zinc ions. This is consistent with the study of Singh et al. that reported that the high affinity site in the repeat region is not sufficient to induce LLPS formation and requires the binding of zinc to low affinity site in the N and C-terminal regions (Singh, Virender, et al.2020). In the same study the authors speculated that at least one of the two cysteines in the repeat region are important for LLPS formation since the substitution of the two cysteines by alanine abrogated LLPS. Another recent study concluded to the importance of the two cysteines in the repeat region in LLPS formation (Gao, Ying-Ying, et al.2022). These two studies were conducted with low zinc concentrations and in the presence of an artificial LLPS inducer, which mask the contribution of low affinity sites. In contrast, our experimental conditions, without artificial LLPS inducer, enabled us to study the impact of zinc binding to the low affinity sites and show their contribution to droplets formation.

Moreover, only the constructs that contained an active R2R3 high-affinity site (xoo-tau and oox-tau), demonstrated the formation of large aggregates. Based on our results, we propose the following model (Fig.6): Two zinc-binding sites participate in

intermolecular bridging, creating a chain of tau molecules held together by zinc ions. Even though the constant of zinc binding to tau is rather low, the disordered structure of tau and the possibility to create long chains of tau molecules glued by zinc lead to the formation of the large entangled and dynamic conglomerate of tau molecules, which we observe as droplets. A similar mechanism through complex-coacervation has recently been described between tau and RNA (Najafi et al. 2021).

Despite recent studies on LLPS of tau, it is still not clear how this process is linked to the pathological aggregation of tau. Our data suggest that these two processes are regulated by Zn^{2+} ions through distinct mechanisms – the formation of droplets needs the presence of any two sites, while zinc-induced tau aggregation needs the active high-affinity site along with one of the low-affinity sites.

Finally, the fact that a very small fraction of tau was found in droplets suggests that nucleation centers are necessary for the initiation of droplet growth. This hypothesis is in good agreement with the fact that upon increase of zinc concentration the size of droplets increases in parallel with the percentage of the tau involved in droplets.

Conclusion

In summary, we confirmed the presence of three zinc binding sites on tau protein, characterized the thermodynamics of zinc binding to each site and provided a model describing the role of each site in the induction of tau aggregation and droplet formation. The molecular mechanism of zinc-induced LLPS and aggregation of tau protein proposed by this study brings new clues to understanding the pathogenesis of tauopathies and paves the way to the conception of new therapeutic strategies for tauopathies.

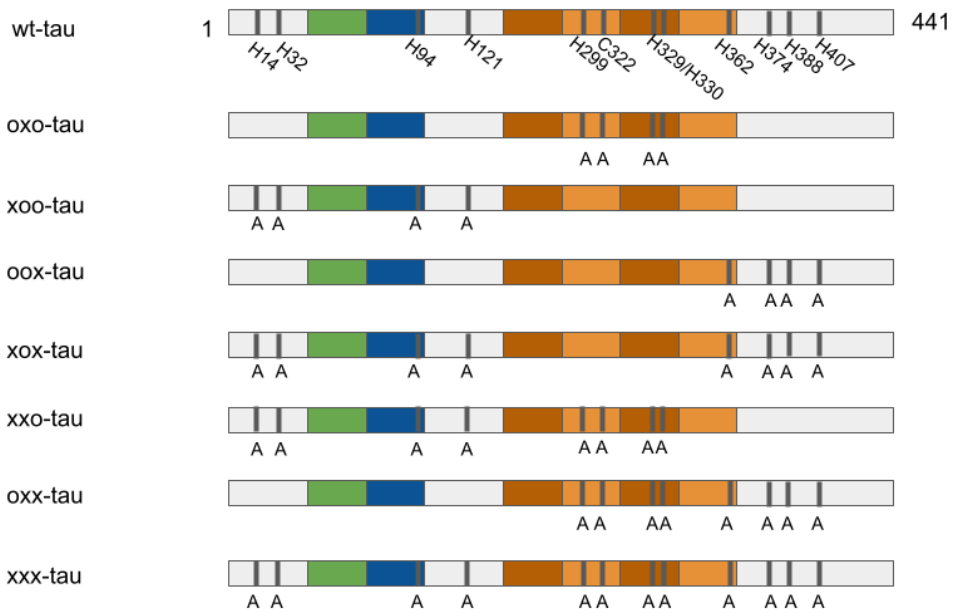

Figure 1. wt-Tau and tau constructs. Cysteines and histidines are marked on the wt-tau sequence, and alanine mutations for each mutant are shown below histidines and cysteines positions.

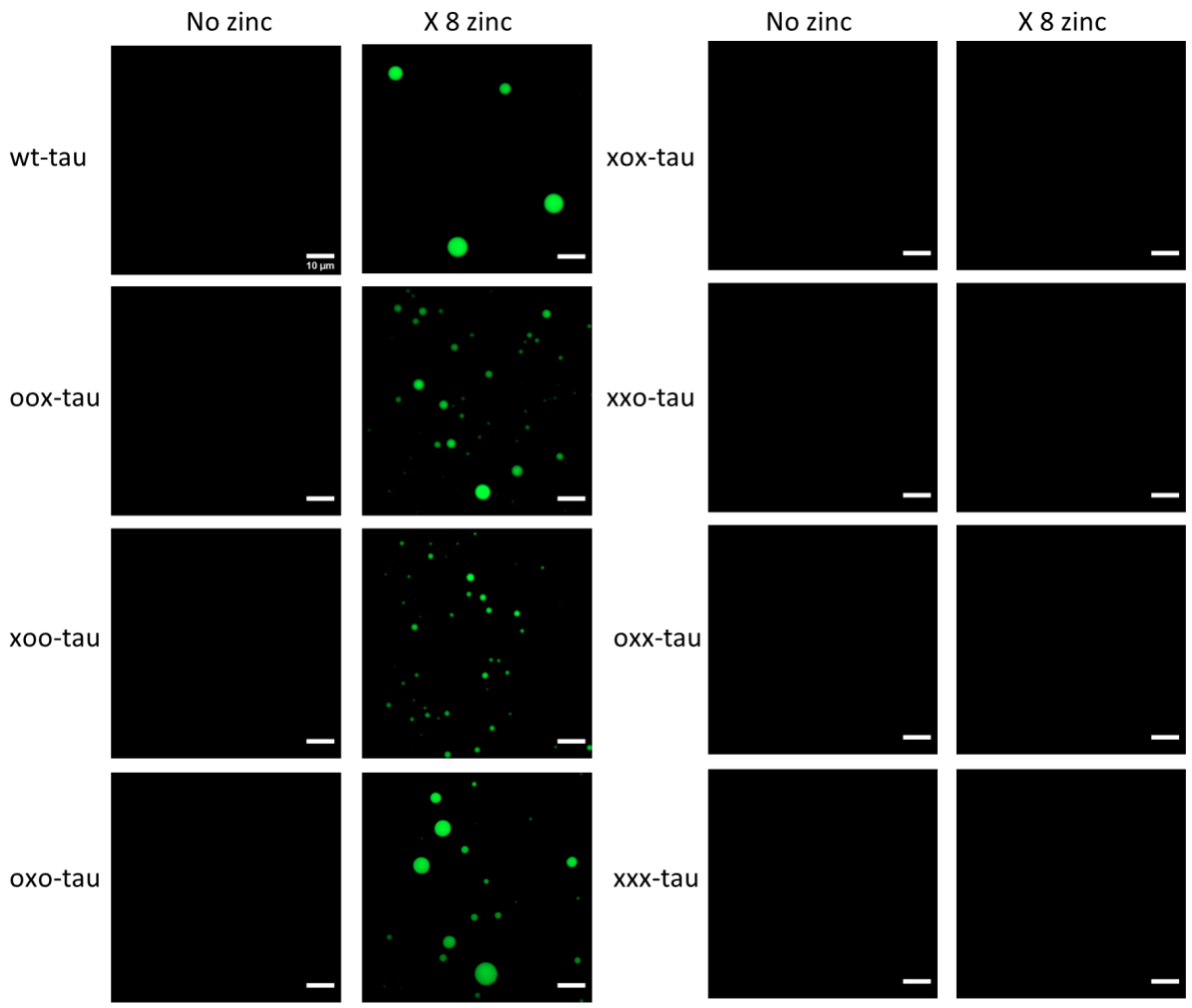

Figure 2. **At least two Zn-binding sites are necessary for LLPS of tau protein.** Representative fluorescence microscopy images of 50 µM wt-tau and different constructs in the absence and presence of 400 µM Zn^{2+} in 50mM Tris 1mM TCEP buffer pH 7.5 at 40°C. Scale bar 10 µm.

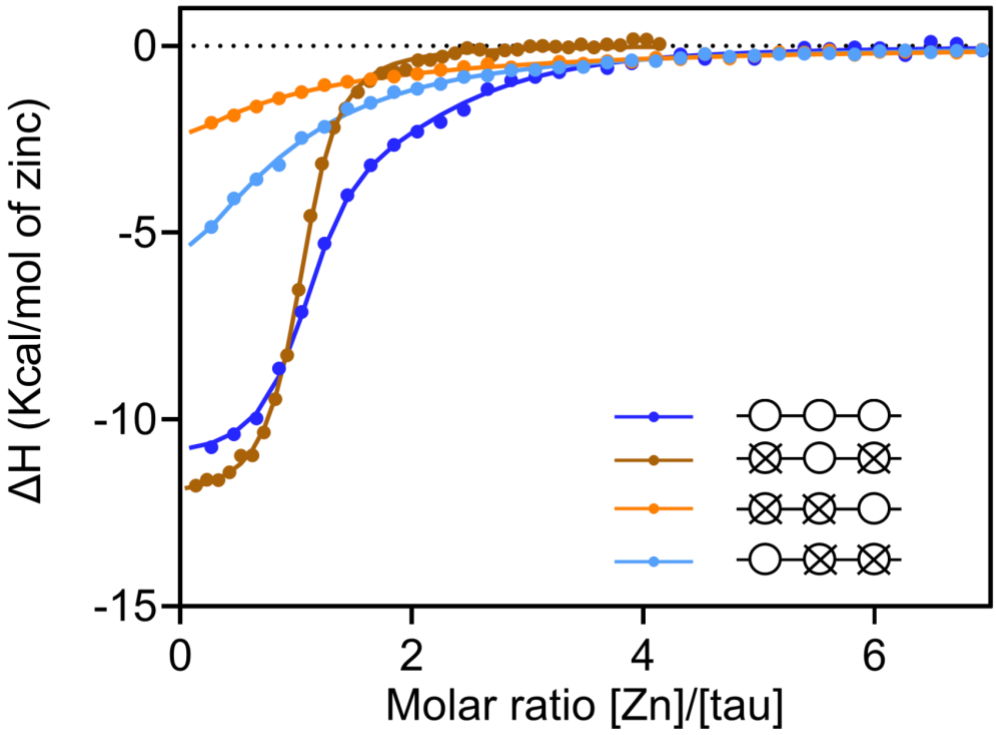

Figure 3. ITC curves of tau-zinc interaction. 50 µM of wt-tau (blue curve) and constructs: xox-tau (brown curve), oxx-tau (light blue curve) and xxo-tau (orange curve) were titrated by zinc in 50 mM tris, 1 mM TCEP pH7.5 buffer at 10°C. Data were fitted with one set of sites model for all mutants and with two sets of sites model for wt-tau.

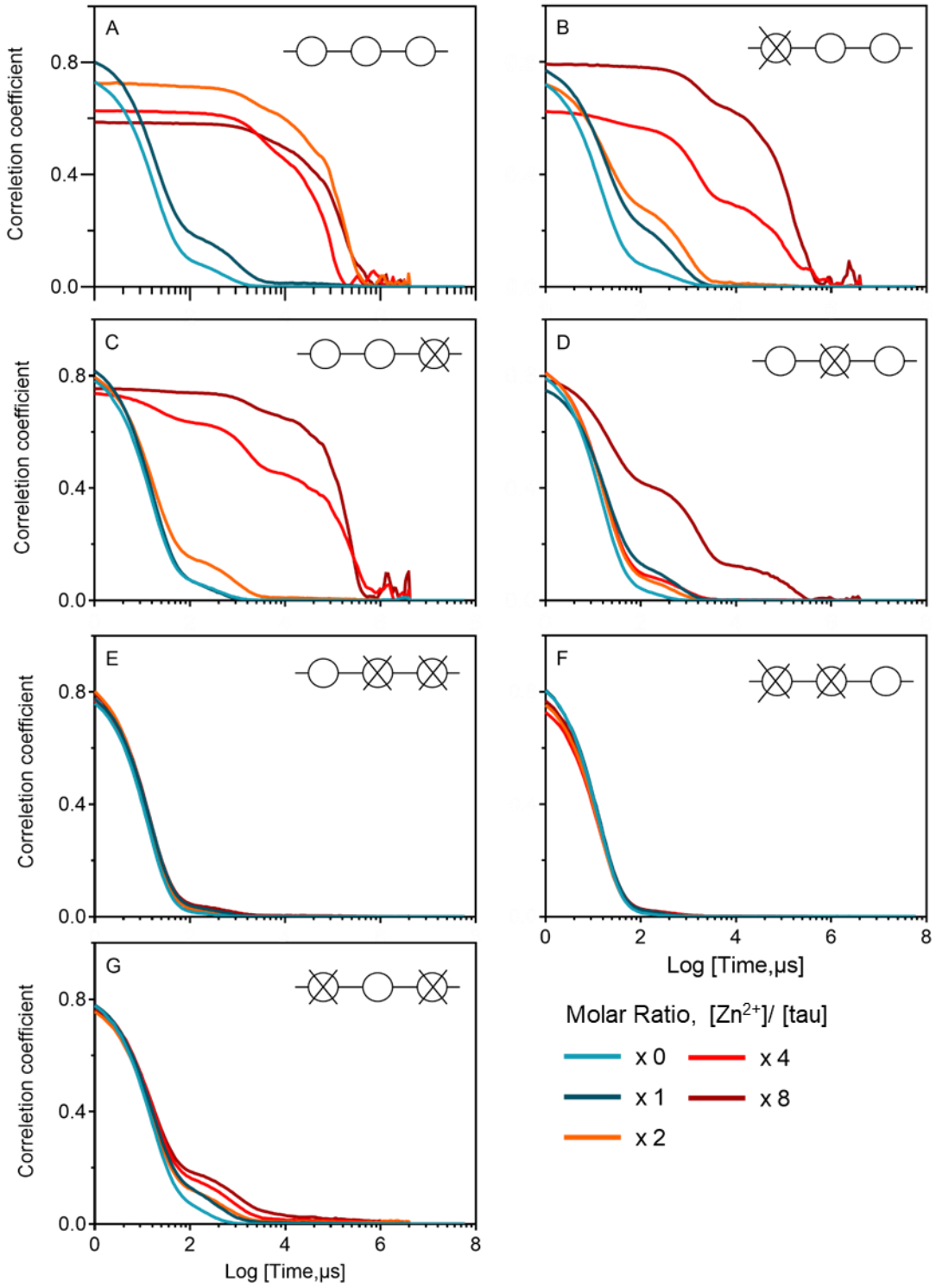

Figure 4. Typical DLS correlation curves of wt-tau and its mutants. 50 µM tau in the absence (blue curve) and presence of 50 (dark blue curve), 100 (orange curve), 200 (red curve) and 400 µM $ZnCl_2$ (brown curve) at 40°C.(A) wt-tau, (B) xoo-tau, (C) oox-tau, (D) oxo-tau, (E) oxx-tau, (F) xxo-tau and (G) xox-tau. For all mutants, experiments were performed at least three times.

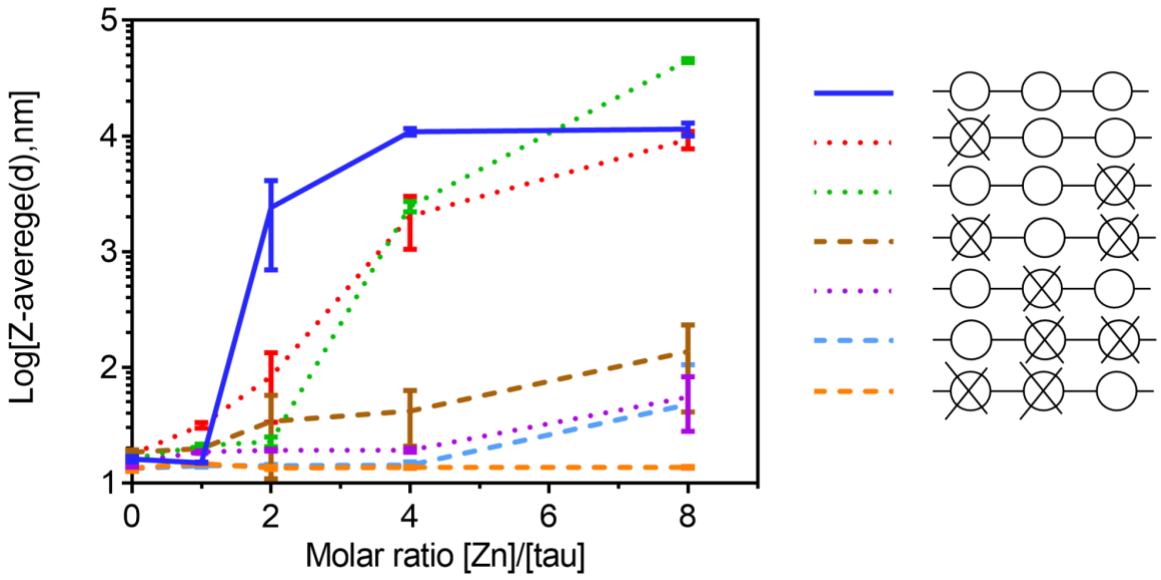

Figure 5. Z-average-mean intensity size for different zinc/tau ratios. Tau concentration is 50 µM. Solid blue line for wt-tau, dotted red line for xoo-tau, dotted green line for oox-tau, dashed brown line for xox-tau, dotted purple line for oxo-tau, dashed light blue for oxx-tau and dashed orange line for xxo-tau. For all mutants, experiments were performed at least three times).

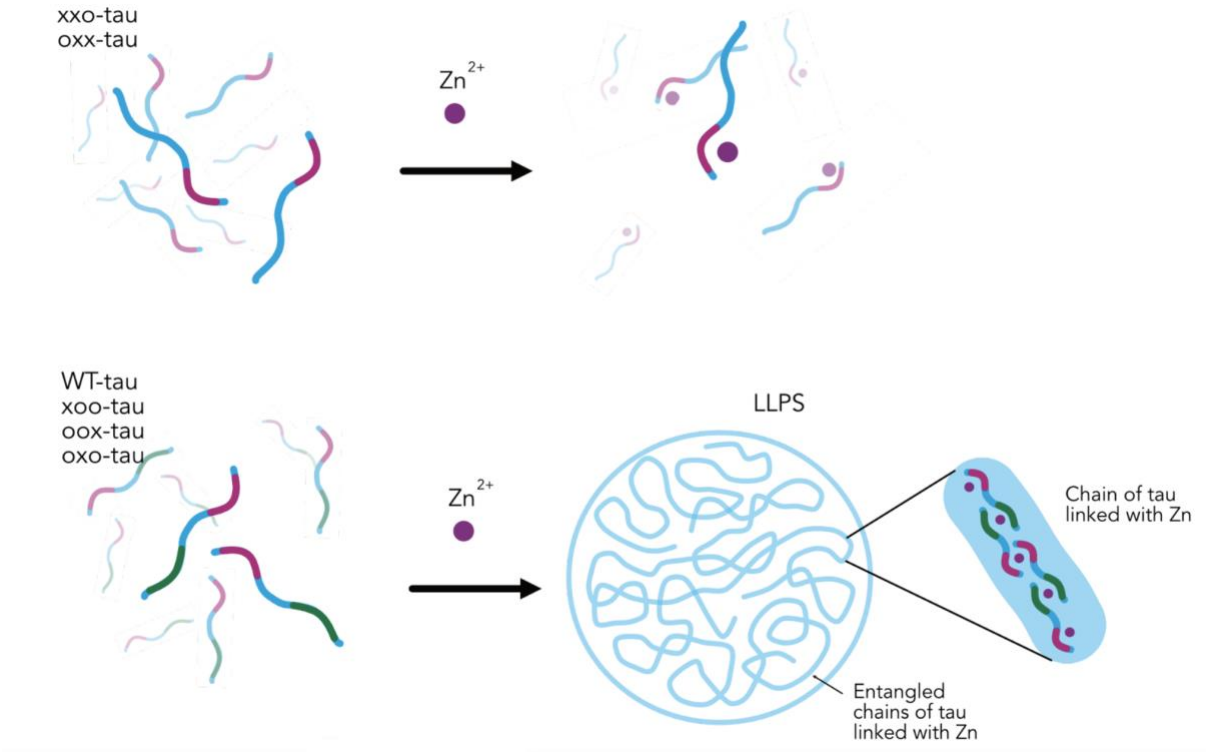

Figure 6. Model of LLPS formation. In the presence of only one site, zinc binds to tau without inducing oligomerization (top panel). In the presence of two sites or more, zinc binding induces the formation of long chains of tau bridged by zinc, leading to the formation of LLPS.

Table 1. Thermodynamic parameters of zinc binding to wt-tau and its mutants obtained by ITC.

Mutant	N	K_a (M^{-1})	ΔH (kcal.mol^{-1})	TΔS (kcal.mol^{-1})
wt-tau**	1.0±0.0 2.0±0.1	$6.7±0.5×10^6$ $2.0±0.2×10^5$	-10.6±0.1 -1.8±0.1	-1.8 5.1
xox-tau*	0.96±0.1	$1.2±0.1×10^6$	-12.2±0.1	-4.6
xxo-tau*	0.95±0.0	$3.3±0.5x10^4$	-4.2±0.2	-1.7
oxx-tau*	0.8±0.1	$2.4±0.2×10^4$	-10.6±0.8	-4.6

* one set of site model; ** two sets of site model.

Table 2. Z-average of wt-tau and its mutant in the presence of different zinc concentrations at 40°C. Z-average is expressed in nm unless otherwise stated. (For all samples, experiments were performed at least three times).

Molar Ratio, $[Zn^{2+}]$/ [tau]	Z-average, d.nm						
	wt-tau	oox-tau	xoo-tau	xox-tau	oxo-tau	xxo-tau	oxx-tau
0	16.0±0.9	16.2±0.8	17.7±0.3	18.5±0.9	15.2±1.5	13.5±0.9	13.3±0.3
1	14.9±0.2	21.1±0.6	31.5±1.8	19.9±0.7	18.5±0.5	14.7±0.4	14.1±0.4
2	2,4±1,7 µm	22.8±2.2	83.4±49.9	34.1±23.2	19.2±0.4	13.5±0.4	14.0±0.3
4	11,4±1,4 µm	2.5±0.2 µm	2.0±1.0 µm	41.9±21.0	19.2±0.8	13.7±0.2	14.3±0.9
8	11,5±1,5 µm	45,1±18,2µm	9,3±1.6 µm	0,1±0,09 µm	0,8±0,03 µm	13.7±0.2	14,6±0.1

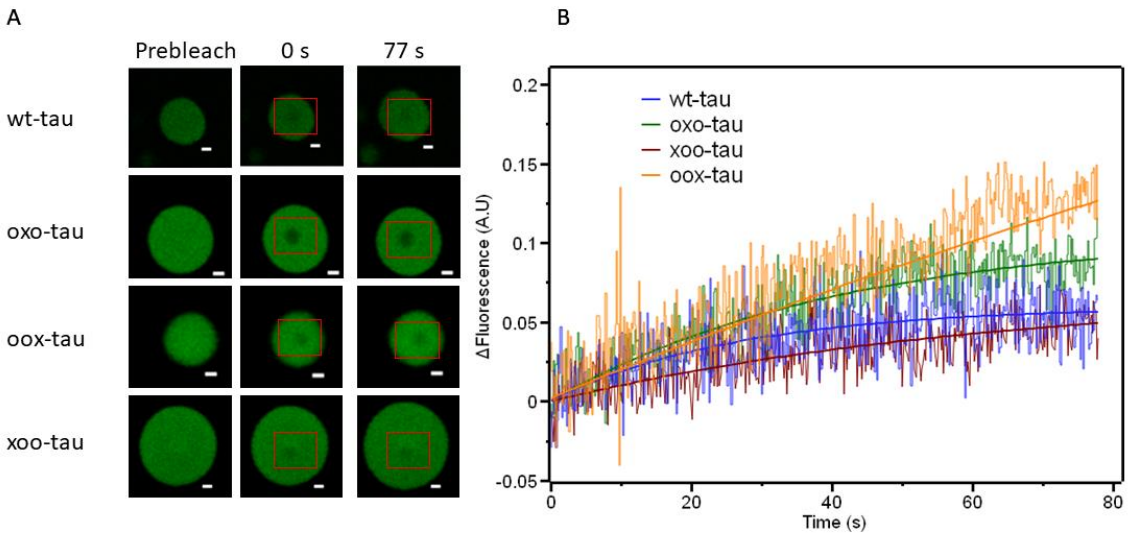

Figure S1. Zinc induced wt-tau and mutants droplets are liquid. (A) FRAP analysis on the selected liquid droplets of 50 µM wt-tau and mutants in the presence of 400 µM $ZnCl_2$ in 50mM Tris 1mM TCEP buffer pH 7.5 at 25°C before, during (0 s) and after photobleaching (77 s). Scale bar 1µm. (B) FRAP traces for droplets of wt-tau (blue curve) and mutants (oxo-tau green curve, oox-tau orange curve and xoo-tau red curve) after inducing LLPS with 400 µM $ZnCl_2$ in 50mM Tris 1mM TCEP buffer pH 7.5 at 25°C.

Supplementary method

Fluorescence recovery after photobleaching (FRAP)- To induce LLPS, Alexa fluor labelled wt-tau and its mutants' samples were prepared by adding zinc ions at 400 µM final concentration to 50 µM labeled tau in 50 mM Tris, 1mM TCEP buffer pH 7.5. FRAP experiments were performed using an SP5 Leica confocal microscope equipped with x 63 oil immersion objective (1.4 numerical aperture). Each experiment started with two image scans, followed by a series of five bleach pulses of a circular area (1.6 µm diameter) within the droplet every 0.173 s using the 488 nm wavelength laser at 80% power and an emission spectra range from 500 to 535 nm. Subsequently, a series of 450 single-section images were collected over 77.8 s. For all constructs at least 5 separate FRAP measurements were performed in two independent experiments, and curves were independently normalized according to the method of Phair *et al*. 2004.

Competing financial interests

The authors declare no competing financial interests.

Credit authorship contribution statement

Dahbia Yatoui: Investigation, Formal analysis, Writing – original draft, Visualization. Philipp O. Tsvetkov: Conceptualization, Formal analysis, Writing – original draft, Validation, Supervision. Romain La Rocca: Investigation. Viktoriia E. Baksheeva: Investigation. Diane Allegro: Resources. Géraldine Ferracci: Investigation. Deborah Byrne: Methodology, Formal analysis. François Devred: Writing – review & editing, Supervision.

Data availability

Data will be made available on request.

Funding

This study was supported by the Algerian ministry of higher education and scientific research (PhD scholarship of Dahbia Yatoui).

Acknowledgements

We acknowledge the support and expertise of the NeuroTimone Platforms (PFNT) of the INP, in particular the Interactome Timone Platforms (PINT), certified by Aix Marseille University (AMIDEX), the CNRS and Inserm and financed in part by the FEDER and Provence-Alpes-Côte d'Azur Région (APR-EX 2016 Neuro-Plasma).

References

Barbier, Pascale, Orgeta Zejneli, Marlène Martinho, Alessia Lasorsa, Valérie Belle, Caroline Smet-Nocca, Philipp O. Tsvetkov, François Devred, and Isabelle Landrieu. 2019. “Role of Tau as a Microtubule-Associated Protein: Structural and Functional Aspects.” *Frontiers in Aging Neuroscience* 11 (August): 204.

Boyko, Solomiia, Xu Qi, Tien-Hao Chen, Krystyna Surewicz, and Witold K. Surewicz. 2019. “Liquid–liquid Phase Separation of Tau Protein: The Crucial Role of Electrostatic Interactions.” *Journal of Biological Chemistry*. https://doi.org/10.1074/jbc.ac119.009198.

Caragounis, Aphrodite, Katherine Ann Price, Cynthia P. W. Soon, Gulay Filiz, Colin L. Masters, Qiao-Xin Li, Peter J. Crouch, and Anthony R. White. 2010. “Zinc Induces Depletion and Aggregation of Endogenous TDP-43.” *Free Radical Biology & Medicine* 48 (9): 1152–61.

Chowdhury, S. Roy, S. Roy Chowdhury, and H. Peter Lu. 2022. “Unraveling the Mechanism of Tau Protein Aggregation in Presence of Zinc Ion: The Earliest Step of Tau Aggregation.” *Chemical Physics Impact*. https://doi.org/10.1016/j.chphi.2021.100060.

Efimova, A. D., R. K. Ovchinnikov, A. Yu Roman, A. V. Maltsev, V. V. Grigoriev, E. A. Kovrazhkina, and V. I. Skvortsova. 2017. “[The FUS protein: Physiological functions and a role in amyotrophic lateral sclerosis].” *Molekuliarnaia biologiia* 51 (3): 387–99.

Esler, W. P., E. R. Stimson, J. M. Jennings, J. R. Ghilardi, P. W. Mantyh, and J. E. Maggio. 1996. “Zinc-Induced Aggregation of Human and Rat Beta-Amyloid Peptides in Vitro.” *Journal of Neurochemistry* 66 (2): 723–32.

Gao, Ying-Ying, Tao Zhong, Li-Qiang Wang, Na Zhang, Yan Zeng, Ji-Ying Hu, Hai-Bin Dang, Jie Chen, and Yi Liang. 2022. “Zinc Enhances Liquid-Liquid Phase Separation of Tau Protein and Aggravates Mitochondrial Damages in Cells.” *International Journal of Biological Macromolecules* 209 (Pt A): 703–15.

Garnier, Cyrille, François Devred, Deborah Byrne, Rémy Puppo, Andrei Yu Roman, Soazig Malesinski, Andrey V. Golovin, Régine Lebrun, Natalia N. Ninkina, and Philipp O. Tsvetkov. 2017. “Zinc Binding to RNA Recognition Motif of TDP-43 Induces the Formation of Amyloid-like Aggregates.” *Scientific Reports* 7 (1): 6812.

Grabrucker, Andreas M., Magali Rowan, and Craig C. Garner. 2011. “Brain-Delivery of Zinc-Ions as Potential Treatment for Neurological Diseases: Mini Review.” *Drug Delivery Letters* 1 (1): 13–23.

Huang, Yunpeng, Zhihao Wu, Yu Cao, Minglin Lang, Bingwei Lu, and Bing Zhou. 2014. “Zinc Binding Directly Regulates Tau Toxicity Independent of Tau Hyperphosphorylation.” *Cell Reports* 8 (3): 831–42.

Hu, Ji-Ying, De-Lin Zhang, Xiao-Ling Liu, Xue-Shou Li, Xiao-Qing Cheng, Jie Chen, Hai-Ning Du, and Yi Liang. 2017. “Pathological Concentration of Zinc Dramatically Accelerates Abnormal Aggregation of Full-Length Human Tau and Thereby Significantly Increases Tau Toxicity in Neuronal Cells.” *Biochimica et Biophysica Acta, Molecular Basis of Disease* 1863 (2): 414–27.

Jiji, A. C., A. Arshad, S. R. Dhanya, P. S. Shabana, C. K. Mehjubin, and Vinesh Vijayan. 2017. “Zn Interrupts R4-R3 Association Leading to Accelerated Aggregation of Tau Protein.” *Chemistry* 23 (67): 16976–79.

La Rocca, Romain, Philipp O. Tsvetkov, Andrey V. Golovin, Diane Allegro, Pascale

Barbier, Soazig Malesinski, Françoise Guerlesquin, and François Devred. 2022. “Identification of the Three Zinc-Binding Sites on Tau Protein.” *International Journal of Biological Macromolecules* 209 (Pt A): 779–84.

Li, Xuexia, Xiubo Du, and Jiazuan Ni. 2019. “Zn Aggravates Tau Aggregation and Neurotoxicity.” *International Journal of Molecular Sciences* 20 (3). https://doi.org/10.3390/ijms20030487.

Moreira, Guilherme G., Joana S. Cristóvão, Vukosava M. Torres, Ana P. Carapeto, Mário S. Rodrigues, Isabelle Landrieu, Carlos Cordeiro, and Cláudio M. Gomes. 2019. “Zinc Binding to Tau Influences Aggregation Kinetics and Oligomer Distribution.” *International Journal of Molecular Sciences* 20 (23). https://doi.org/10.3390/ijms20235979.

Mo, Zhong-Ying, Ying-Zhu Zhu, Hai-Li Zhu, Jun-Bao Fan, Jie Chen, and Yi Liang. 2009. “Low Micromolar Zinc Accelerates the Fibrillization of Human Tau via Bridging of Cys-291 and Cys-322.” *The Journal of Biological Chemistry* 284 (50): 34648–57.

Najafi, Saeed, Yanxian Lin, Andrew P. Longhini, Xuemei Zhang, Kris T. Delaney, Kenneth S. Kosik, Glenn H. Fredrickson, Joan-Emma Shea, and Songi Han. 2021. “Liquid-Liquid Phase Separation of Tau by Self and Complex Coacervation.” *Protein Science: A Publication of the Protein Society* 30 (7): 1393–1407.

Ochalek, Anna, Balázs Mihalik, Hasan X. Avci, Abinaya Chandrasekaran, Annamária Téglási, István Bock, Maria Lo Giudice, et al. 2017. “Neurons Derived from Sporadic Alzheimer’s Disease iPSCs Reveal Elevated TAU Hyperphosphorylation, Increased Amyloid Levels, and GSK3B Activation.” *Alzheimer’s Research & Therapy* 9 (1): 90.

Portbury, Stuart D., and Paul A. Adlard. 2017. “Zinc Signal in Brain Diseases.” *International Journal of Molecular Sciences* 18 (12). https://doi.org/10.3390/ijms18122506.

Roman, Andrei Yu, François Devred, Deborah Byrne, Romain La Rocca, Natalia N. Ninkina, Vincent Peyrot, and Philipp O. Tsvetkov. 2019. “Zinc Induces Temperature-Dependent Reversible Self-Assembly of Tau.” *Journal of Molecular Biology* 431 (4): 687–95.

Shelkovnikova, T. A., A. A. Kulikova, F. O. Tsvetkov, O. Peters, S. O. Bachurin, V. L. Bukhman, and N. N. Ninkina. 2012. “[Proteinopathies--forms of neurodegenerative disorders with protein aggregation-based pathology].” *Molekuliarnaia biologiia* 46 (3): 402–15.

Wang, Lu, Ya-Ling Yin, Xin-Zi Liu, Peng Shen, Yan-Ge Zheng, Xin-Rui Lan, Cheng-Biao Lu, and Jian-Zhi Wang. 2020. “Current Understanding of Metal Ions in the Pathogenesis of Alzheimer’s Disease.” *Translational Neurodegeneration* 9 (April): 10.

Wegmann, Susanne, Bahareh Eftekharzadeh, Katharina Tepper, Katarzyna M. Zoltowska, Rachel E. Bennett, Simon Dujardin, Pawel R. Laskowski, et al. 2018. “Tau Protein Liquid-Liquid Phase Separation Can Initiate Tau Aggregation.” *The EMBO Journal* 37 (7). https://doi.org/10.15252/embj.201798049.